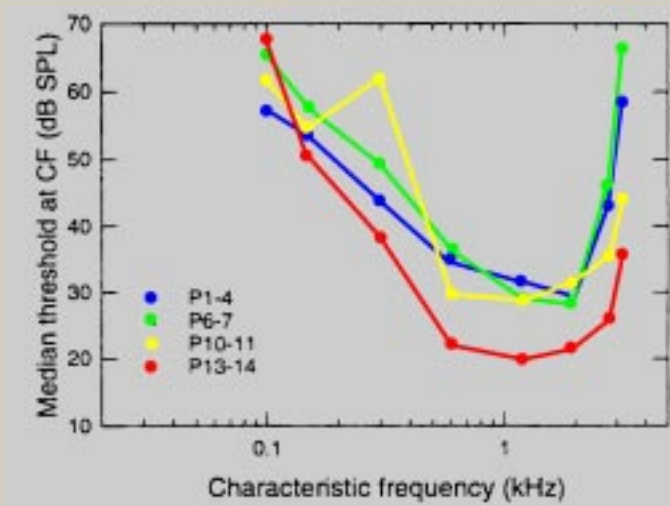


BACKGROUND

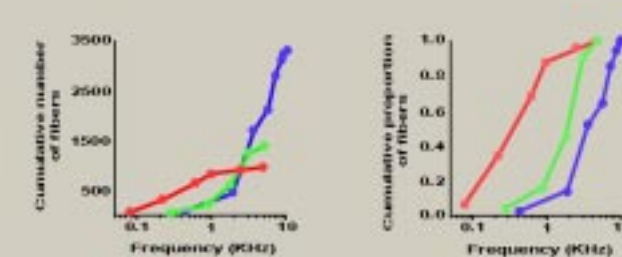


The avian cochlear nucleus laminaris (NL) is the first to receive binaural input and is responsible for computing interaural time differences (ITDs). The organization of NL can either have a plesiomorphic and/or apomorphic pattern, as in the chick and barn owl. We have studied the emu which is a ratite and member of the group Paleognathae. Ratites are a monophyletic group of closely related species (Cracraft, 1974; Sibley and Ahlquist, 1981) whose inner ear morphology show features that are believed to be primitive.



Emus show behaviors associated with specialization for detecting low frequency sounds. These animals make “booming” calls through the resonant help of a long inflated air sac in the neck, parallel to the trachea and connected to it through a narrow slit (Welty, 1979). Emu audiograms (left - Koepl 1998) show that these animals thresholds suggestive of a low frequency specialist.

Koepl et al (1998) showed that emus have a comparatively massive neural representation of frequencies below 1 kHz (right), where even absolute fiber numbers in this region are considerably above those in the other species reported. This again, presumably reflects the behavioral importance of its very low-frequency adult calls (Marchant and Higgins, 1990).



Although previously argued that this species are representative of birds with primitive hearing, we here suggest the these animals are actually specialized for detecting low frequencies and therefore do not show the usual plesiomorphic auditory brainstem organization but are indeed showing an apomorphic pattern. Therefore a plesiomorphic form of NL (monolayer) contains derived neuronal morphologies, where cells show bipolar structure with secondary and tertiary dendritic tufts throughout the nucleus.

Supported by: The work was supported by NIH DCD 00436 to CEC, NINDS/NRSA to KMM and NIHR03DC04382 JZS.

METHODS

ANATOMY

Four peri-hatch Emus were anesthetized with Ketamine (15 mg/kg IM) followed by an overdose of pentobarbital (35 mg/kg IM). After intercardiac injection of heparin, emus were transcardially perfused with saline and fixed by 4% paraformaldehyde in 0.1 M phosphate buffer (PB, pH 7.4). Brains were postfixed overnight and cryoprotected in 30% sucrose in PB at 4°C. Good histological preservation was achieved without a marked loss of antigenicity using these fixatives. The brains were sectioned on a freezing microtome at 30µm thickness.

Antibodies against Parvalbumin, Kv3.1 and SV2 were used with standard immunocytochemical procedures. The avidin-biotin-peroxidase complex (ABC, Vector Labs) was used. Sections were preincubated for one hour in 0.01 PBS buffer with 4% normal goat serum and 0.4% Triton-X, then incubated overnight in the appropriate antibody (1:1000). Sections were incubated for 10 minutes in 3% H₂O₂ in PBS, washed, incubated for one hour in biotinylated secondary antibody diluted at 1:1,000, washed, incubated in ABC for one hour, washed for 20 minutes in PBS followed with 20 minutes in chromagen buffer. Tissue sections were developed using diaminobenzidine tetrahydrochloride (DAB, 0.48 mg/ml); and 0.03% H₂O₂ in Acetate-Imidazole buffer with Nickel sulfate (26.3 mg/ml). Floating sections were mounted on chrom-alum subbed slides, dehydrated, cleared, and coverslipped with Permount. Some cases were additionally counterstained with neutral red. Sections were examined using light microscopy techniques. For double labeled sections the same protocol was used as above but direct secondary was used (RITC or 1:100).

PHYSIOLOGY

Slice preparation. Emus aged E42-P0 of unknown sex were used for field recordings and whole-cell patch recordings. Approximately a 2-4 cm section of brainstem was removed from the embryos following decapitation and immediately placed in oxygenated ACSF (artificial cerebrospinal fluid: in mM: 130 NaCl, 3 KCl, 2 MgCl₂, 26 NaHCO₃, 2 CaCl₂, 1.25 NaH₂PO₄, dextrose). The brainstem was carefully dissected from the skull cavity, discarding the cerebellum. Transverse slices, cut 300-400 µm thick, were cut on a vibrating tissue slicer, and placed in a holding chamber with continuously oxygenated ACSF at room temperature. For experiments, the slices were transferred to a recording chamber, immobilized with a nylon-strung 'harp' and superfused with normal ACSF at a rate of ~2ml/min. All data shown were recorded at room temperature (~22°C), except one: during temperature experiment, the ACSF temperature was controlled with a Warner Instruments in-line heater. Temperatures were recorded from the digital readout of a temperature probe placed in the rear of the recording chamber, and corrected for an ~2°C difference measured in our configuration, between the location of the slice and the placement of the probe. In two experiments, a low-calcium, high magnesium ACSF (same as normal except: 0.5 mM CaCl₂, 3.5 mM MgCl₂) used to test calcium dependence of the evoked field events.

Field recordings. Field recordings were made with a glass microelectrode (~1MΩ) filled with normal ACSF, and Axon Instruments Axoclamp 2B amplifier. Nucleus laminaris, nucleus magnocellularis and the fiber tracts between them were clearly visible at low power (x10 objective on Zeiss Axoskop 2), making electrode placement straightforward. Evoked potentials were stimulated with metal tungsten bipolar electrodes placed in the fibers coming from the ipsilateral NM or in the ipsilateral NM itself, and placed in the contralateral cross-tracts at the midline, or closer to the ventral side of NL. We used a Grass stimulus isolation unit and pulse generator, and evoked responses at a rate of ~1Hz. We were able to successfully record consistent, clear, evoked potentials, with both contralateral and ipsilateral stimulation, from 5-11 sites along the mediolateral axis of the nucleus laminaris in 3 slices, and from 2 sites in 1 slice. Response peaks in contralaterally evoked potentials were often easy to distinguish from the stimulus artifact and the spike potential, while in ipsilaterally evoked potentials the synaptic peak was merged with the spike volley peak and thus obscured.

Whole cell recordings. We made 5 successful whole cell recordings from NL neurons in 3 separate slices. We used glass microelectrodes with pipette resistances of 5-8 MΩ, filled with intracellular recordings solutions containing (in mM: 120 potassium gluconate, 20 KCl, 0.1 EGTA, 2 MgCl₂, 2 Na₂ATP, 10 HEPES; also included 0.2-0.5% lucifer yellow or sulfarhodamine). Individual cells were visualized using IR-DIC optics under 40x magnification and using a CCD camera and monitor system, and recorded with an Axoclamp 2B amplifier. All recordings were digitized at 10-20 kHz with Axon Instruments (Union City, CA) software (PCLamp 7) and hardware (Digidata 1200 A-to-D board) and a PC. Data were later analyzed using IGOR Pro scientific analysis software (Wavemetrics, Lake Oswego, OR). One NL neuron was successfully stained with lucifer yellow.

MODEL

The model emulates an array of neurons, each with an adjustable number of dendrites, a soma, and an axon with an axon hillock, a myelinated segment, and a node of Ranvier. Each section has an adjustable number of equipotential compartments. All geometric, electrical, and channel parameters are adjustable, as are the number of synapses/dendrite, the synaptic locations, and the distribution of synaptic locations. Channel types include potassium (high and low voltage activated [Kv3.1, 1.1] and delayed rectifier), sodium, and passive. Values were obtained from physiological studies of NM and NL in chick. Voltage dependent channels are specified by Hodgkin-Huxley-like parameters. Each neuron in the array feeds into a single inhibitory neuron, which feeds back onto all neurons in the array. The stimulus is a pure tone of adjustable frequency, with adjustable interaural phase difference.

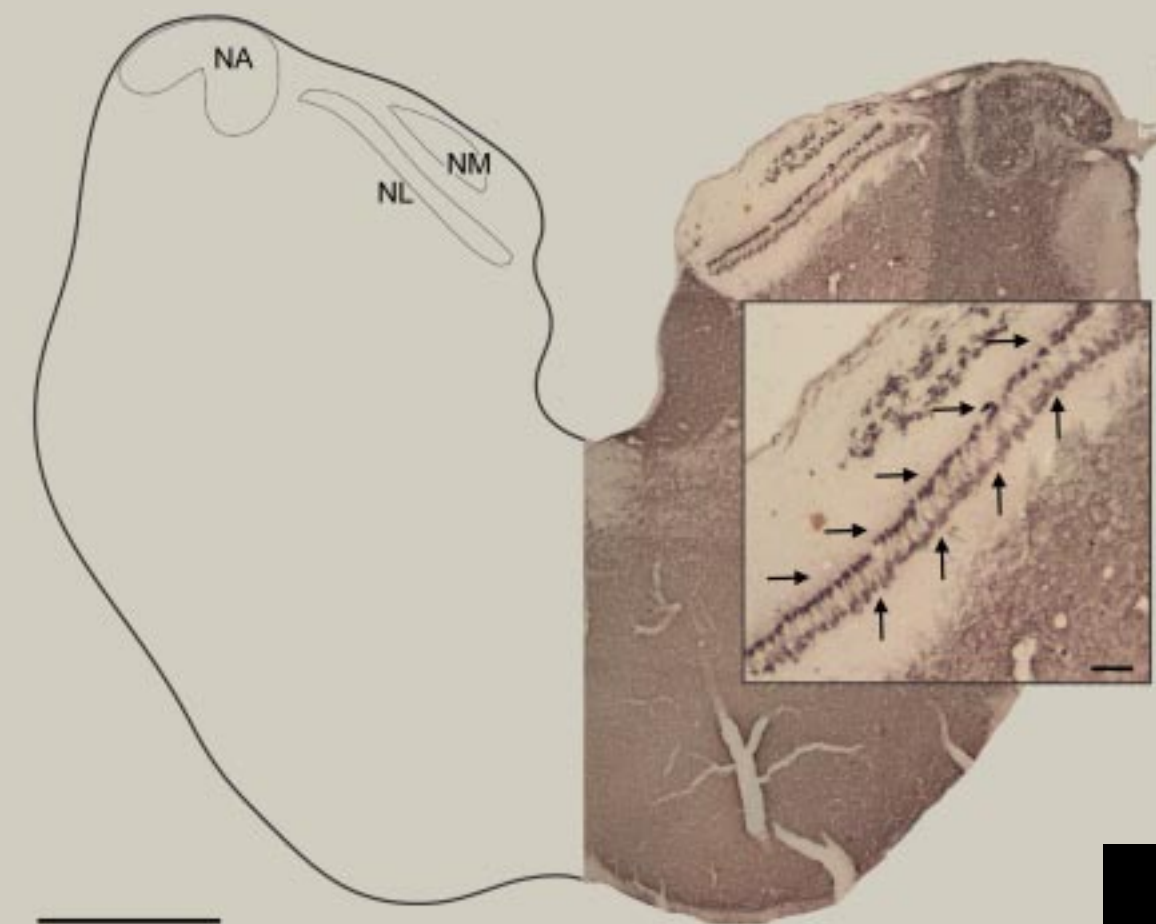
The synapses fire with conductance proportional to an alpha-function, with adjustable time constant, peak conductance, and reversal potential. The excitatory synapses fire as individual Poisson processes, with probability rate given by a modified sinusoid, with adjustable amplitude and vector strength. The inhibitory neuron is a simple integrate-and-fire type.

The implementation uses the program NEURON and has a graphical user interface for controlling the parameters and running the model. NEURON provides a real-time display of data and analysis including the potential at various locations, the two stimuli, the synaptic firings, spike counters, period histograms of synaptic firings and the action potentials, and their vector strengths.

ANATOMICAL RESULTS SUGGEST MORPHOLOGICAL SPECIALIZATION

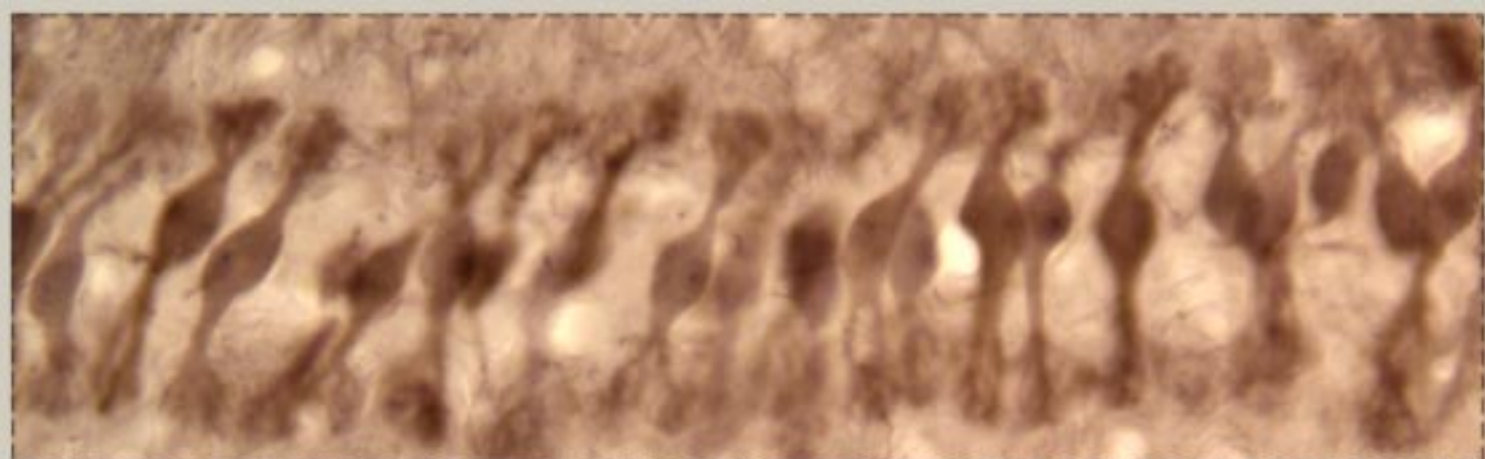


← **Figure 1.** Diagram of emu brain showing the plane of sections for all studies presented.

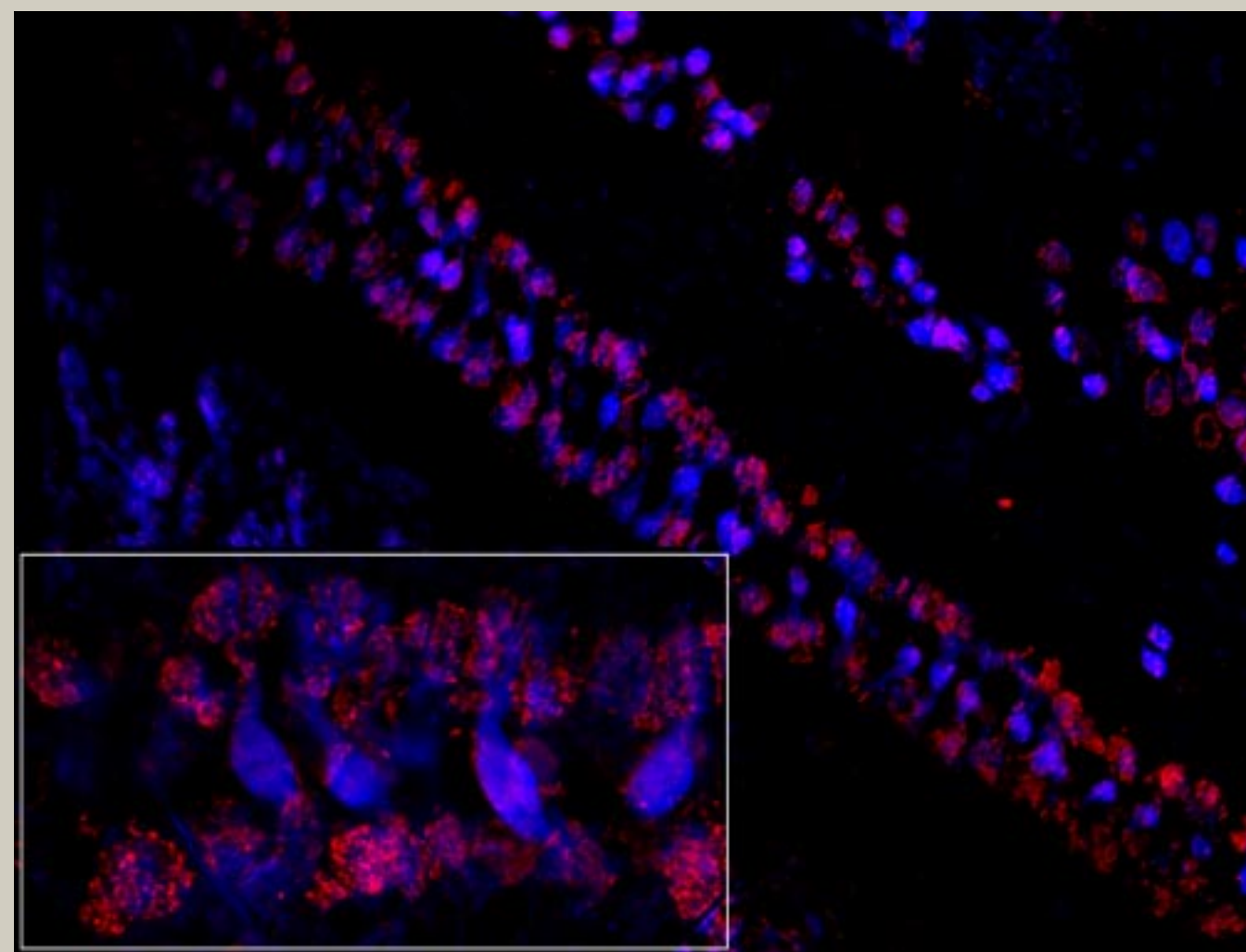
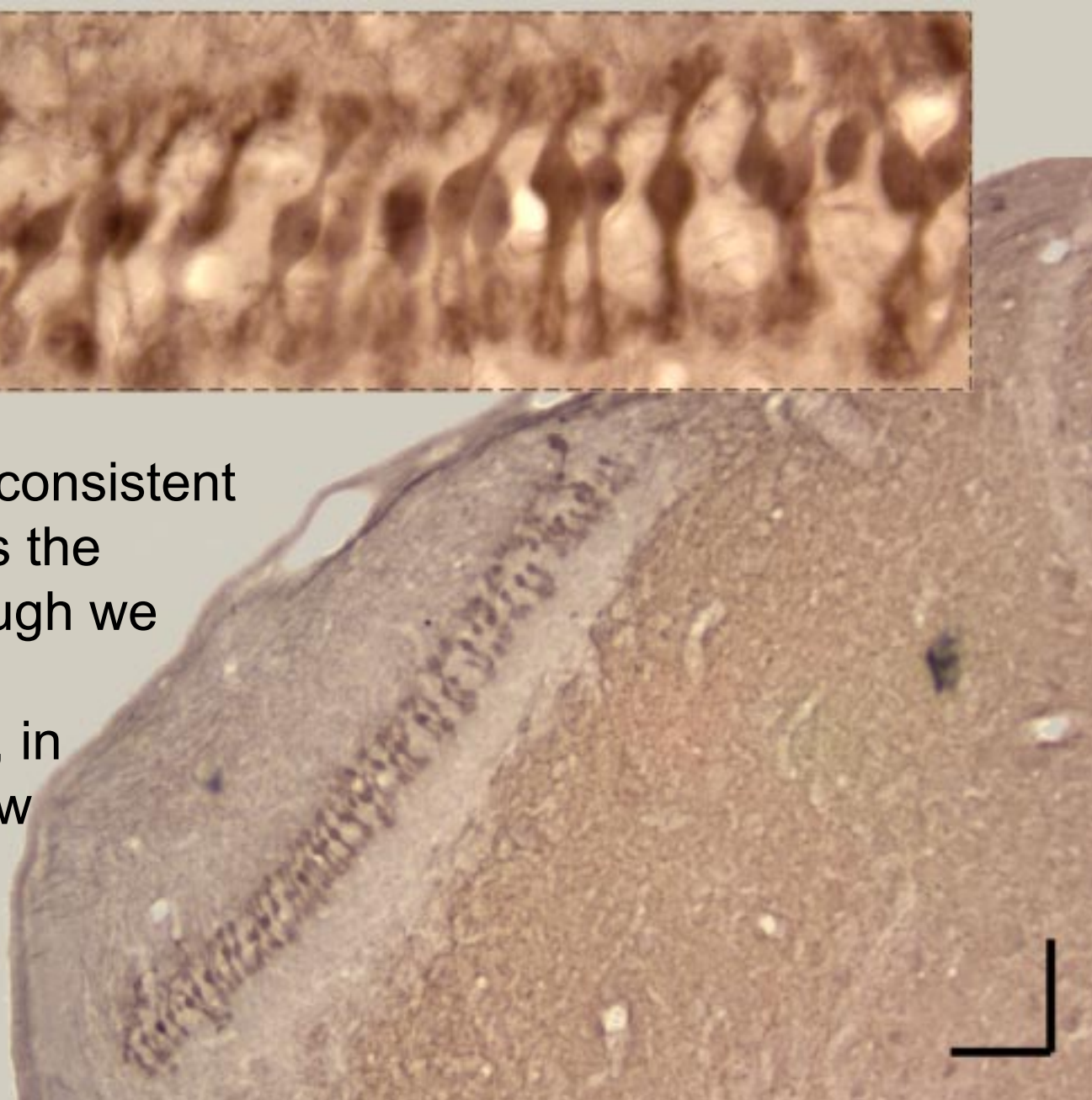


← **Figure 2.** Synaptic vesicle protein 2 (SV2) Immunoreactivity with corresponding diagram of the organization of the auditory brainstem. Note that precipitation product is segregated to the neuropil of NL (arrows, insert)

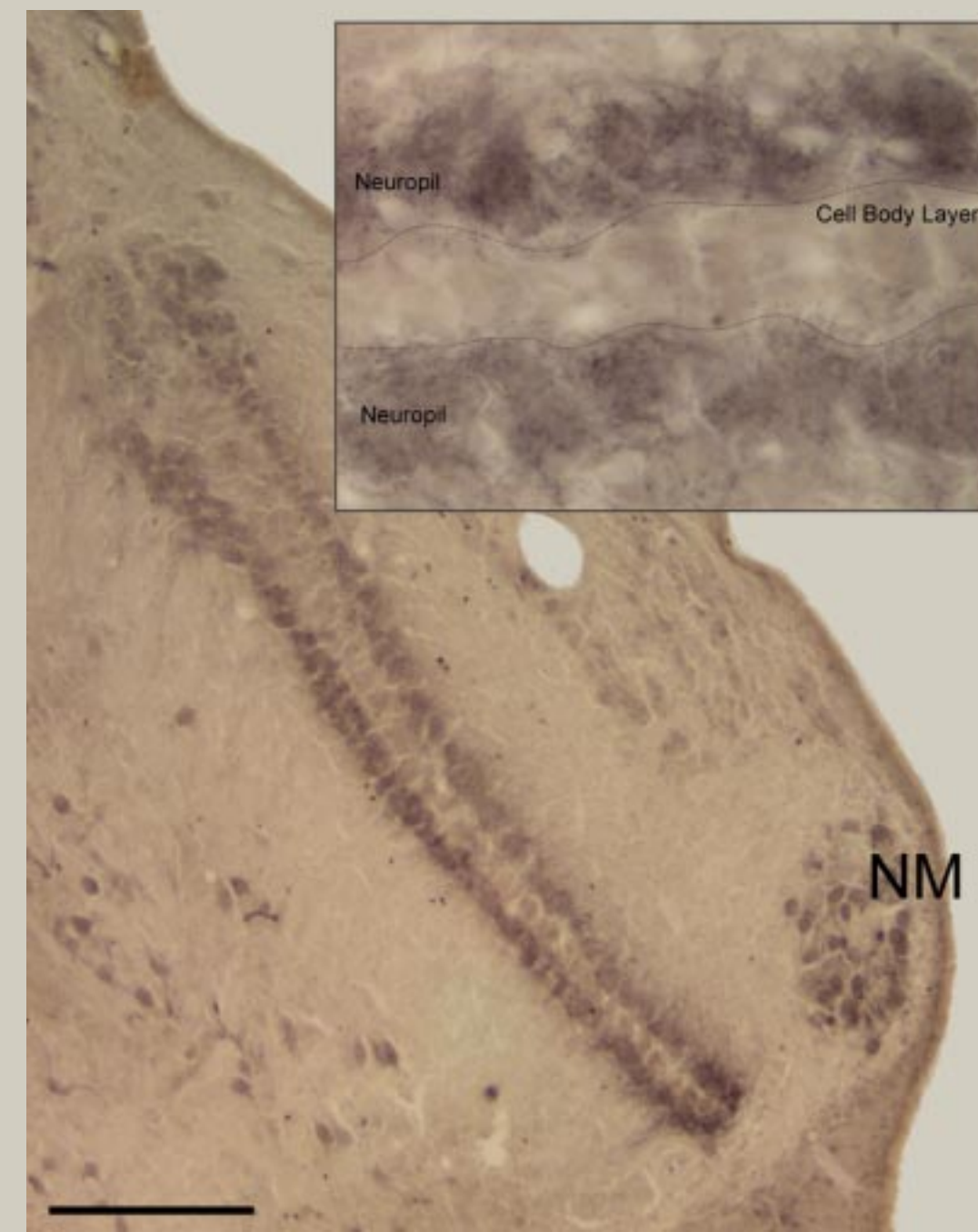
Figure 4. Parvalbumin Immunoreactivity. Insert shows a magnification of NL neurons in



the same section. Note the consistent dendritic morphology across the medial lateral extent. Although we do not show data for the frequency distribution in NL, in all birds ever examined show a high-medial to low-lateral tonotopic organization. Dorsal is up medial is left.



↑ **Figure 3.** Double labeled NL neurons. Red: SV2, Blue: parvalbumin. Insert shows same section at higher magnification. Note that SV2 is restricted to tufted endings.



↑ **Figure 5.** Expression of Kv3.1 protein in NM and NL. High threshold K⁺ channels like Kv3.1 produce delayed rectifier like currents. They activate rapidly between -10 mV and -20 mV and have rapid activation and deactivation kinetics. In the emu NL, the neuropil on either side of the monolayer of cell bodies was intensely immunoreactive. This neuropil includes the dorsal and ventral dendrites of NL neurons as well as the terminal arbors of NM axons. Somata were clearly outlined by Kv3.1 immunolabel (insert).

OTHER LOW FREQUENCY ARCHOSAURS NL NEURONS LACK OF DENDRITIC TUFTS

CHICKEN
Auditory generalist. Plesiomorphic organization - monolayer. Neurons show dendritic length gradients from high CF (short) to low CF (long). No tufts.

BARN OWL
Auditory specialist with emphasis at higher CF (up to 12kHz) Apomorphic organization - not a monolayer. Majority of neurons have short dendrites but lead to longer dendrites at lower CF. No tufts.

ALLIGATOR
Auditory generalist ??? audiograms and vocalization suggest emphasis on lower CF (1kHz and below). Plesiomorphic organization - monolayer. But neurons located at highest CF show bipolar morphology with thick primary dendrites. No tufts

EMU
Auditory specialist ??? audiograms and vocalization suggest emphasis on lower CF (1 kHz and below). Plesiomorphic organization, a monolayer but all neurons show thick primary dendrites with tufted endings. Possible plesiomorphic organization with apomorphic neurons.

PHYSIOLOGICAL RECORDINGS SHOW LATENCY SHIFTS AND SINGLE SPIKING NEURONS.

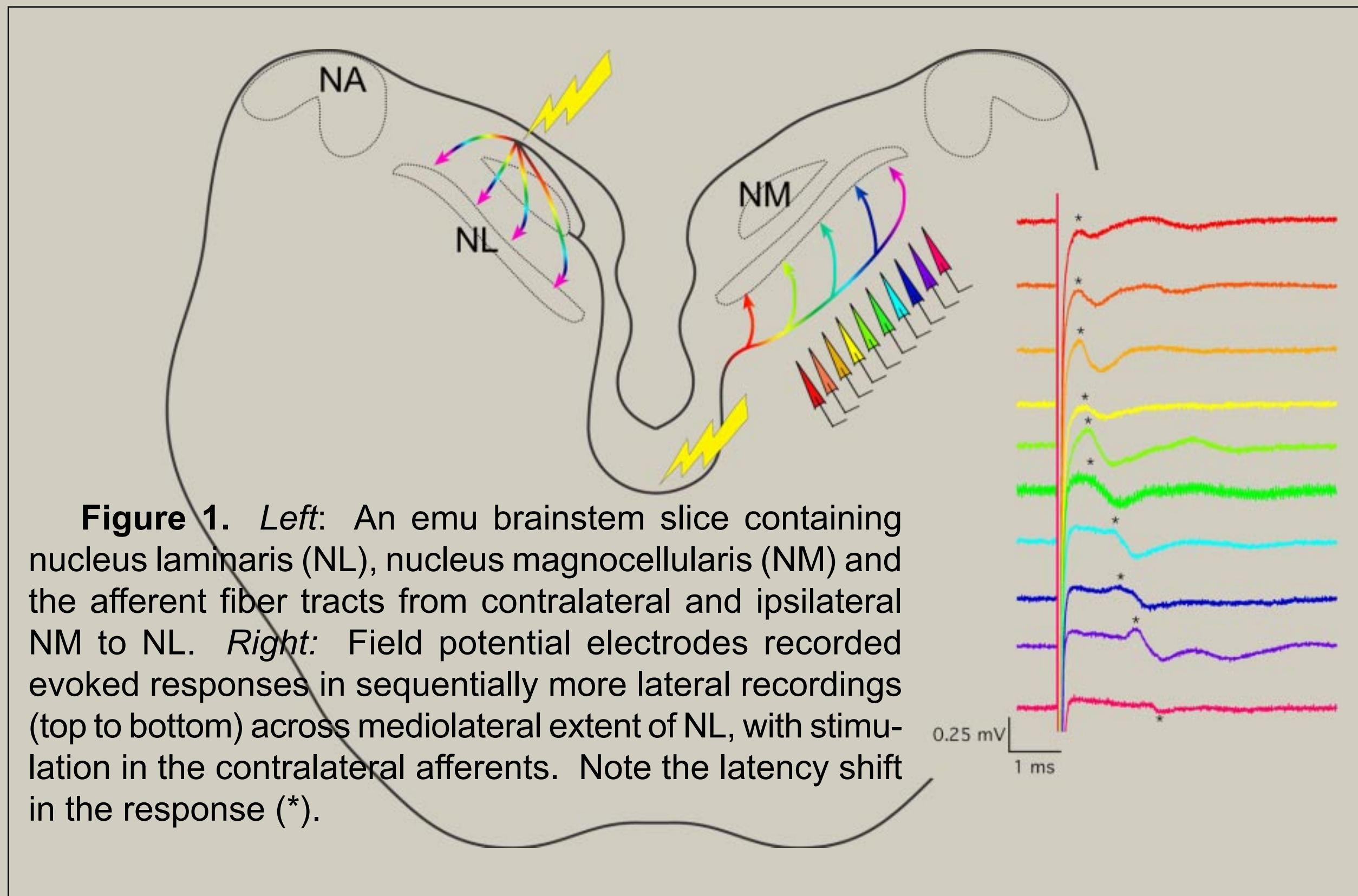


Figure 1. *Left:* An emu brainstem slice containing nucleus laminaris (NL), nucleus magnocellularis (NM) and the afferent fiber tracts from contralateral and ipsilateral NM to NL. *Right:* Field potential electrodes recorded evoked responses in sequentially more lateral recordings (top to bottom) across mediolateral extent of NL, with stimulation in the contralateral afferents. Note the latency shift in the response (*).

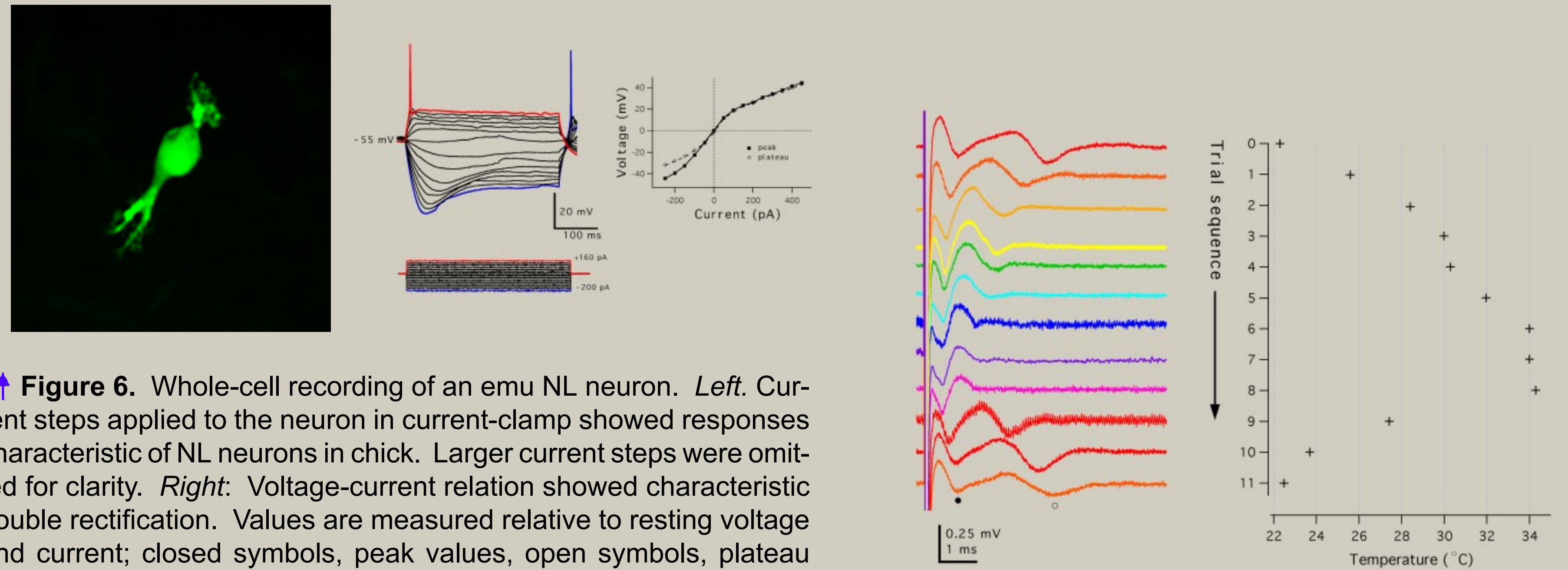


Figure 6. Whole-cell recording of an emu NL neuron. *Left:* Current steps applied to the neuron in current-clamp showed responses characteristic of NL neurons in chick. Larger current steps were omitted for clarity. *Right:* Voltage-current relation showed characteristic double rectification. Values are measured relative to resting voltage and current; closed symbols, peak values, open symbols, plateau values. *Far left:* Lucifer yellow fill of NL neuron.

Figure 5. Effect of temperature on evoked response. *Top left:* 11 sequential trials, top to bottom, during bath temperature manipulation. *Top right:* Measured temperature (x-axis) for each trial (y-axis) as it was increased, then decreased to room temperature. *Bottom:* Measured peak latency decreases linearly with increasing temperature.

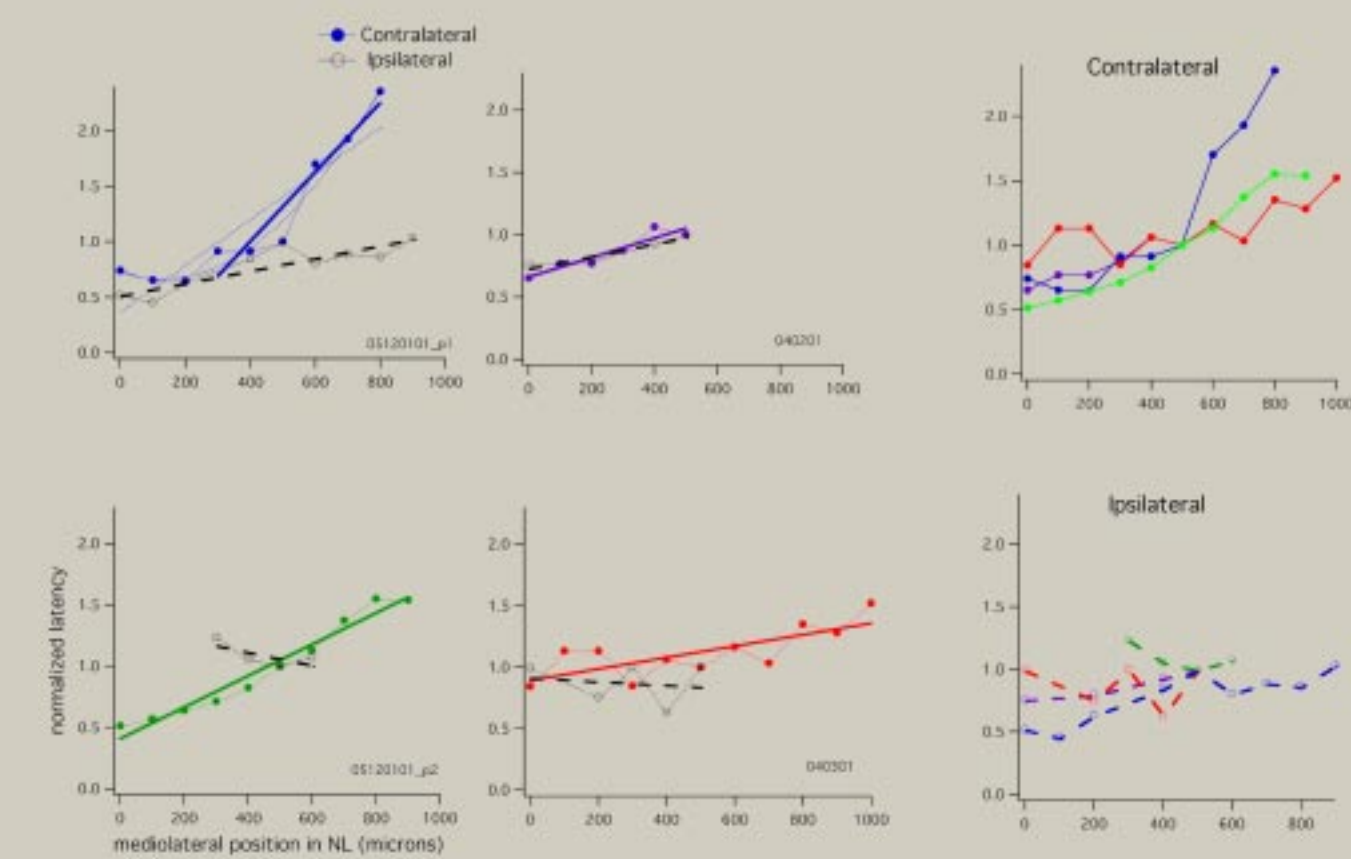


Figure 2. Latency of late component of evoked responses versus mediolateral recording position in NL (0 is most medial). *Left:* Four plots show ipsilaterally (open circles) and contralaterally (filled circles) evoked responses recorded in a sequence of mediolateral positions (n = 3 slices; two peaks are from the same recording.) Latencies are normalized to that measured approximately 500 μm from medial edge of NL for each contra or ipsi data set for each peak. Raw normalizing latencies in ms (contra, ipsi): top left: (0.64, 0.55), bottom left: (1.3, 0.87), topright: (1.1, 0.9), bottom right: (1.07, 0.88).

Right: Replot of the same data, grouped by stimulation.

Figure 3. Maximal shifts in latency is greater for contralaterally evoked responses than for ipsilaterally. Latency shift values are derived from the slopes of the delay line fits in Figure 2.

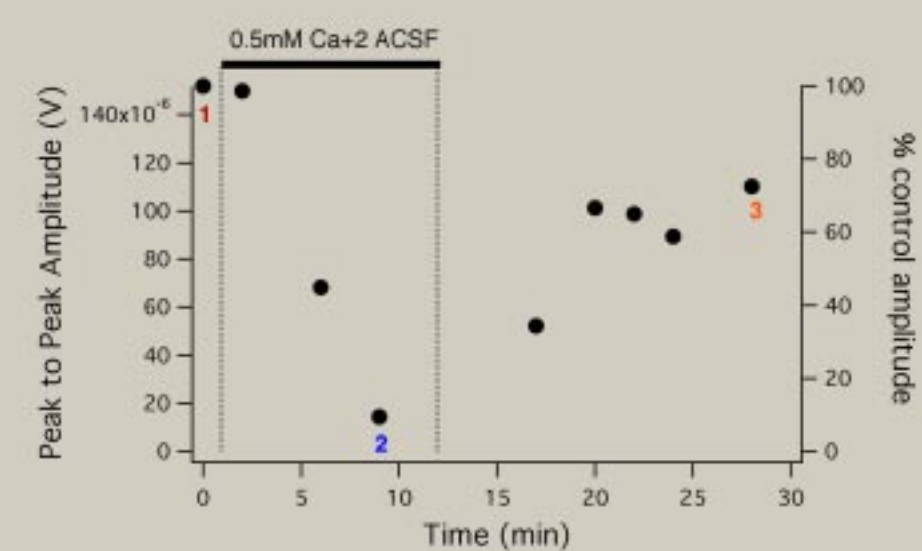
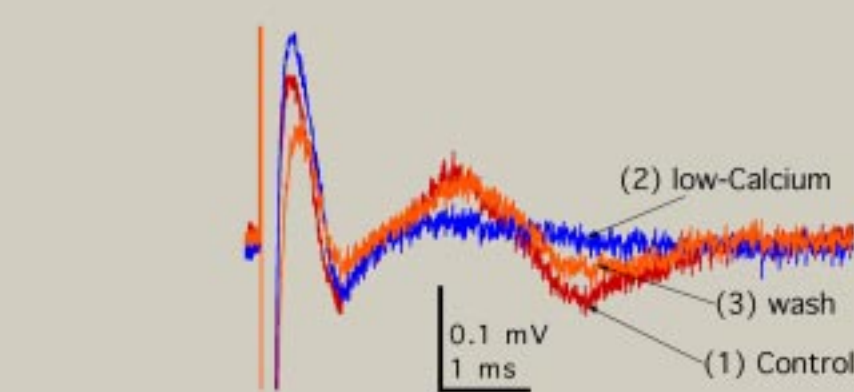
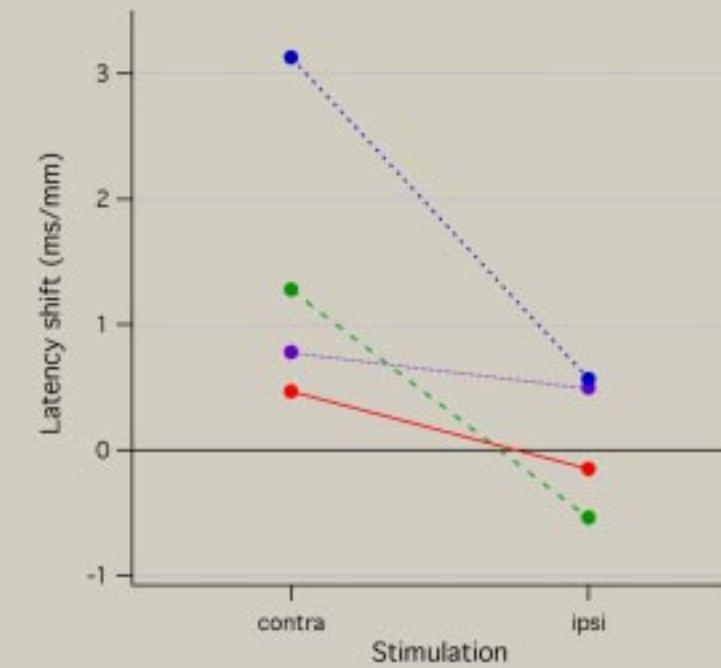


Figure 4. Removal of calcium from the ASCF eliminates the late component of the evoked response, suggesting a synaptic origin of this peak. *Top:* Traces from control, low-calcium (0.5mM), and wash conditions. *Bottom:* Time course of the change in peak-to-peak amplitude of the late component.

Are there delay lines in emu nucleus laminaris? Evoked field potentials from emu NL (Figs 1-3) showed a pronounced, consistent variation in latency across the medial-to-lateral extent of NL (up to ~3 ms per mm) when stimulated contralaterally, consistent with the idea of delay line input; this effect was less pronounced or absent with ipsilateral stimulation.

Late component of evoked response is calcium dependent. A stable field recording response was evoked using contralateral stimulation in normal ACSF (control, Fig 4). A low-calcium (0.5mM) solution was washed in (calcium washout), reducing the peak-to-peak amplitude of the late component to <15% its initial value. A return to normal calcium (2mM) resulted in the return of the late component to ~80% its initial value. These results suggest the late component is synaptic in origin.

Peak latency is temperature dependent. A linear decrease in latency of both the early and late components is observed with increasing temperature (range: 22-34°C)(Fig 5). This relationship was determined to have a Q10 of ~1.8 (Q10 is defined as the factor by which the latency increases with every 10°C increase in temperature.)

Whole cell recordings of emu NL neuron. We recorded from neurons of the NL in whole cell recording mode (n=5; Fig 6). Current steps applied to a neuron in NL revealed physiological behavior similar to classic NL responses in chick: only a single spike is evoked, even with large current steps (larger steps not shown), inward rectification with depolarization, prominent 'sag' with hyperpolarization (outward rectification) and an anode-break spike. Interestingly, there are noticeable (sometimes quite large, >10mV) spontaneously occurring PSPs.

A NEURON MODEL YIELDS GOOD ITD CODING AT LOW BEST FREQUENCIES

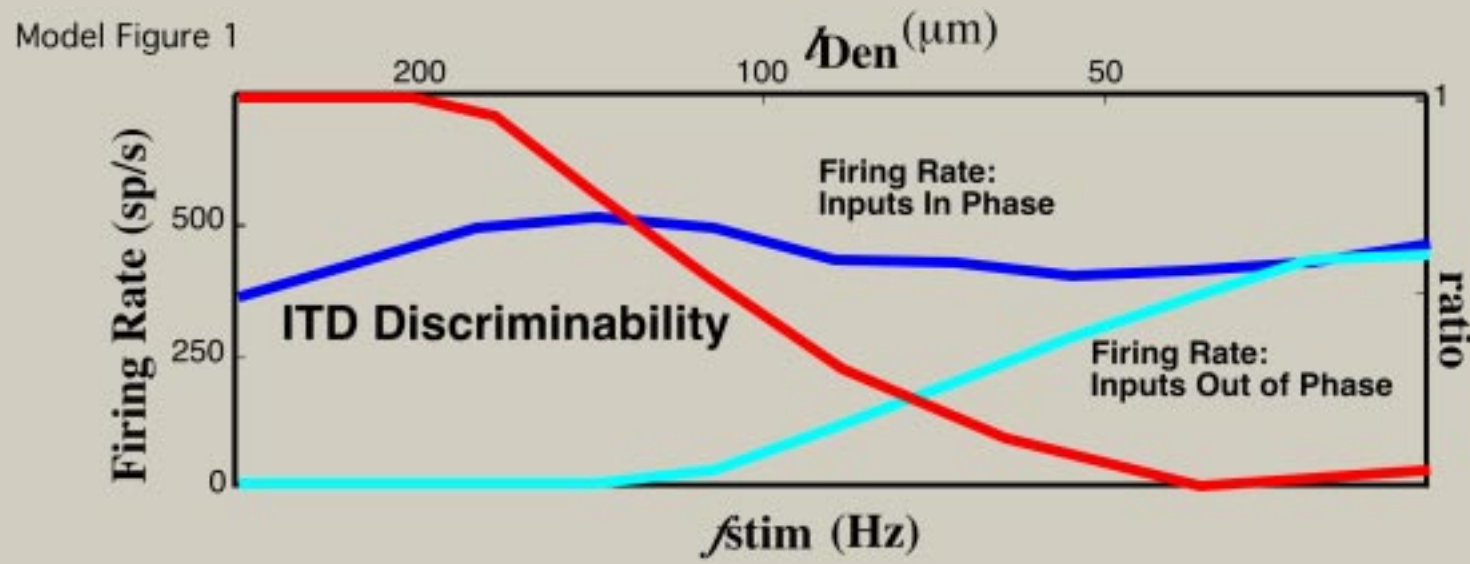


Figure 1. High firing rate for in-phase inputs contrasted with low firing rate for out-of-phase inputs gives good ITD discriminability (red curve high). High firing rate for in-phase inputs combined with high firing rate for out-of-phase inputs gives poor ITD discriminability (red curve low).

Figure 2. ITD discriminability is enhanced when all the synapses are concentrated in the most distal 40% of the dendrite (over the case when all the synapses are uniformly distributed over the entire dendrite). The enhancement at the lowest frequencies is here masked by ceiling effects: it does not appear in the phase tuning curve at those frequencies.

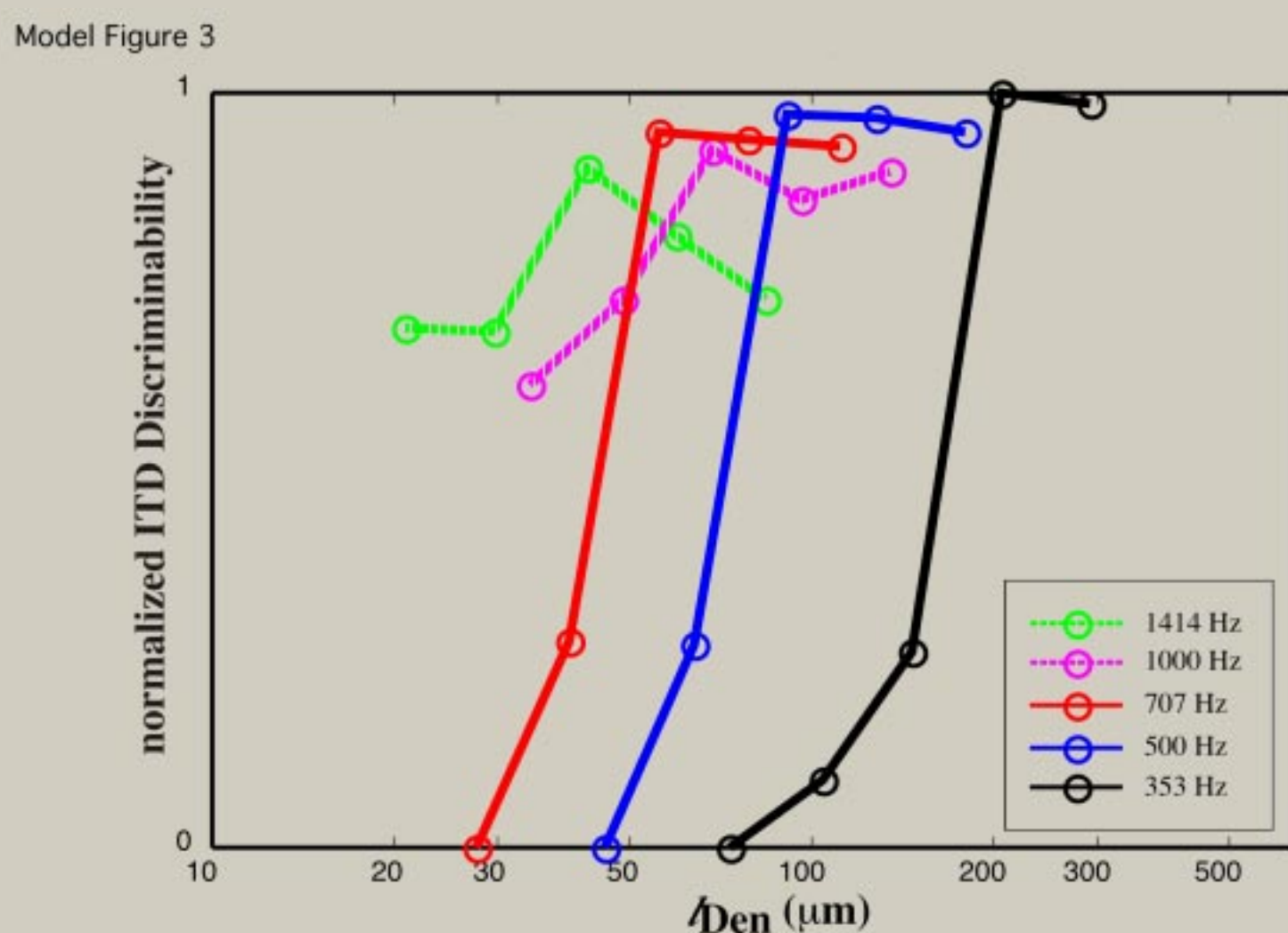
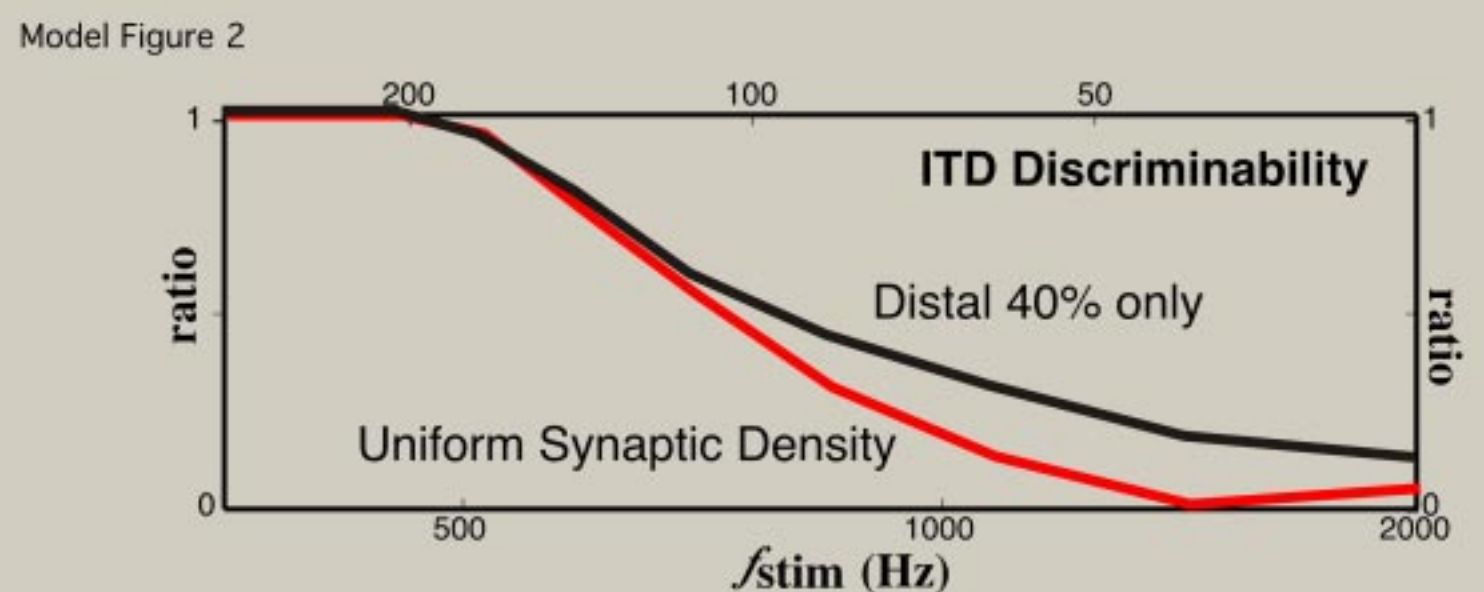


Figure 3. For every stimulus frequency, the ITD discriminability of the NL neuron increases with increasing dendritic length, until a maximum (optimal) length is reached. The optimal length is longer for low frequencies than high frequencies, thus predicting that lower frequency tuned NL neurons will be longer than higher frequency NL neurons. A low frequency specialist will have many more long dendrites than short dendrites.

CONCLUSIONS:

We made field recordings across the mediolateral extent of NL and evoked responses by stimulating the ipsilateral or contralateral fibers (Physiology Figure 1). With contralateral stimulation we found a consistent shift in response latency across the mediolateral extent of the NL (Physiology Figures 1-2), with a maximal shift ranging from 0.47 to 3.13 ms/mm. Ipsilateral stimulation evoked responses which had more variable latencies; the shift in latency with mediolateral position in NL was much less pronounced (n=2 peaks) or showed a negligible or negative shift (n=2), with maximal shifts ranging from -0.54 to 0.56 ms/mm (Physiology Figure 3).

Anatomically, NL consists of a monolayer of neurons in the emu, with polarized dendritic arbors oriented dorsally and ventrally. These neurons show prominent thick primary dendrites, with tufted endings. This pattern seems apomorphic in that the inputs are segregated to the dendritic tufts. This can be seen when using an antibody against synaptic vesicle protein and calcium buffer protein (SV; Parvalbumin; Anatomy Figure 1-3).

These results fit the predictions of a biophysical model of NL neurons. The model demonstrates that for low frequency inputs, ITD tuning is enhanced by increasing electrotonic isolation of the synapses from the soma. This can occur by segregating inputs on dendritic tufts of long dendrites rather than spacing the inputs uniformly along entire dendritic length (as occurs in chick).

Although emus belong to the Eoaves group, the organization of the coincidence detector circuit appears derived and suited to low frequency ITD detection.

REFERENCES

J Cracraft *Phylogeny and evolution of the ratite birds*. Ibis (1974) 116:494-521
 M L Hines and NT Carnevale. *The NEURON Simulation Environment*. Neural Computation 9 (1997), 1179-1209. See <<http://www.neuron.yale.edu>>.
 C Koppl, O Gleich, G Schwabedissen, E Siegl and GA Manley. *Fine structure of the basilar papilla of the emu: implications for the evolution of avian hair-cell types*. Hear Res 1998 Dec;126(1-2):99-112
 C Koppl, A Wegscheider, O Gleich and GA Manley. *A quantitative study of cochlear afferent axons in birds*. Hear Res. 2000 Jan;139(1-2):123-43.
 S Marchant and PJ Higgins, *Dromaius novaehollandiae*. In: *Handbook of Australian, New Zealand and Antarctic Birds, Vol. 1 (Ratites to Ducks)*. Oxford University Press, Melbourne, pp. 47-58.
 EM Overholt, EW Rubel and RL Hyson. *A circuit for coding interaural time differences in the chick brainstem*. J Neurosci. 1992 May;12(5):1698-708.
 CG Sibley and JE Alquist *The phylogeny and relationships of the birds as indicated by DNA-DNA hybridization*
 JZ Simon, CE Carr and SA Shamma. *A Dendritic Model of Coincidence Detection in the Avian Brainstem*. Neurocomputing (1999), 26-27, 263-269.
 JC Welty *The Life of Birds* (1979) pp209.